Reactions between Vanadium Ions and Biogenic Reductants of Tunicates: Spectroscopic Probing for Complexation and Redox Products *in Vitro*†

Daniel E. Ryan,*,‡ Kathryn B. Grant,‡ Koji Nakanishi,‡ Patrick Frank,§ and Keith O. Hodgson§

Department of Chemistry, Columbia University, New York, New York 10027, Department of Chemistry, Stanford University, and Stanford Synchrotron Radiation Laboratory, Stanford, California 94305

Received September 8, 1995; Revised Manuscript Received April 25, 1996⊗

ABSTRACT: Several species of marine tunicates store oxygen-sensitive V^{III} in blood cells. A sensitive colorimetric V^{III} assay was used to survey the leading candidates for the native reducing agent of vanadate in tunicates (i.e., An-type tunichromes, glutathione, NADPH, and H_2S) in reactions with V^V or V^{IV} ions under anaerobic, aqueous conditions at acidic or neutral pH. Except for the case of An-1 and V^V ions in pH 7 buffer, the assay results for the biogenic reducing agents clearly showed that appreciable quantities of V^{III} products were not generated under the conditions tested. Therefore, the assay results place new limits on hypothetical mechanisms of V^{III} formation *in vivo*. For reactions between An-1 and V^V ions in pH 7 buffer, low levels of V^{III} products could not be ruled out because of an interfering peak in the colorimetric assays. For similar reactions between V^V ions and An-1, or an An-1,2 mixture, in mildly to moderately basic media, the product mixtures precipitated as greenish black solids. Analyses of the precipitated V/An mixtures using vanadium K-edge X-ray absorption spectroscopy (XAS) showed that the major products were tris(catecholate)-type V^{IV} complexes ($65 \pm 6\%$) and bis(catecholate)-type $V^{IV}O$ complexes ($20 \pm 4\%$). XAS analysis of the V/An-1 product mixture also provided evidence of a minor V^{III} component ($9 \pm 5\%$ of total V), notable for possible relevance to tunicate biochemistry. The combined results of XAS studies, spectrophotometric studies [Ryan, D. E., et al. (1996) *Biochemistry 35*, 8640−8650], and EPR studies [Grant, K. B., et al. (1996) *J. Inorg. Biochem.* (manuscript in preparation)] consistently establish that reactions between tunichromes (Mm-1 or An-1) and V^V ions generate predominantly V^{IV}−tunichrome complexes in neutral to moderately basic aqueous media.

Several species of marine tunicates are known for their accumulation of vanadium ions in blood cells. Tunicates of the suborder Phlebobranchia are intruiguing for their ability to reduce V^V ions collected from sea water to the oxygen-sensitive V^{III} state (Hawkins et al., 1983). In sea water (pH ca. 8.3), V^V is present as monomeric vanadate ions ($H_2VO_4^-/HVO_4^{2-}$, $pK_a = 8.3$). After transport into the blood cells of *Ascidia nigra* and *Ascidia ceratodes*, for example, the cellular vanadium is at least 90% V^{III} and ≤10% V^{IV} according to magnetic susceptibility, X-ray absorption, and SQUID[1] measurements (Boeri & Ehrenberg, 1954; Tullius et al., 1980; Lee et al., 1988a; Frank et al., 1995). The vanadium oxidation states have also been studied by EPR (Dingley et al., 1981; Hawkins et al., 1983; Frank et al., 1986) and by cytological staining (Rezaeva et al., 1964; Brand et al., 1989). Oxygen-sensitive V^{III} must be kept in a reducing environment in the blood cells; however, the blood plasma is aerobic to some extent and carries V^V (Anderson & Swinehart, 1991).

As the standard reduction potential E^o for the V^{IV}/V^{III} couple is 0.337 V (volts vs NHE; Lide, 1993), the generation of V^{III} in blood cells must be mediated by a potent reducing agent. Candidates for the native reducing agent include tunichromes **1** (Chart 1), a family of yellow, polyphenolic tripeptides prevalent in blood cells of phlebobranchs (Bruening et al., 1985; Oltz et al., 1988). In *A. nigra* blood, for example, tunichromes **1** and vanadium ions are both present in morula-type blood cells, and tunichromes constitute up to 50% of morula cell dry weight (Oltz et al., 1989). In studies of tunichrome−vanadium chemistry *in vitro*, reactions between the simplest tunichrome, Mm-1 **2a**, and V^V ions under various conditions generated V^{IV} complexes in neutral media and free V^{IV} ions in acidic media (Ryan et al., 1996). Although the Mm-type tunichrome **2a** (from an Fe-accumulating stolidobranch) did not generate V^{III} products, the An-type tunichromes **1** from V-accumulating phlebobranchs possess a nonconjugated DOPA or TOPA residue (ring C of **1**) that could conceivably play a role in producing V^{III}. Two-electron oxidation of the C ring could complete π-conjugation in An-type tunichromes via tautomerization (Scheme 1) and may thermodynamically drive

† These studies were supported by National Research Service Award GM 14042 (D.R.), NIH GM 08281 (K.G.), NIH GM 10187 (K.N.), and NSF CHE 94-23181 and NIH RR-01209 (K.O.H.). XAS experiments were conducted at SSRL, which is supported by the Department of Energy, Office of Basic Energy Sciences, Divisions of Chemical and Materials Sciences. Further support to SSRL is provided by the National Institutes of Health, National Center for Research Resources, Biomedical Research Technology Program and by the Department of Energy, Office of Health and Environmental Research.

* To whom correspondence should be addressed.

‡ Columbia University.

§ Stanford University.

⊗ Abstract published in *Advance ACS Abstracts,* June 1, 1996.

[1] Abbreviations: acac, acetylacetonate; Boc, *tert*-butoxycarbonyl; *iso*-Bu, *iso*-butyl; cat, catechol; DOPA, 3,4-dihydroxyphenylalanine; DTT, dithiothreitol; edtaH_2, ethylenediaminetetraacetic acid, dibasic; EPR, electron paramagnetic resonance spectroscopy; EXAFS, extended X-ray absorption fine structure; GSH, glutathione; GSSG, glutathione disulfide; Me, methyl; NADPH, nicotinamide adenine dinucleotide phosphate, reduced form; NHE, natural hydrogen electrode; HPLC, high-performance liquid chromatography; LUMO, lowest unoccupied molecular orbital; NMR, nuclear magnetic resonance spectroscopy; salen, *N,N*′-ethylenebis(salicylideniminato); SQUID, super quantum interference device; TBDMS, *tert*-butyldimethylsilyl; THF, tetrahydrofuran; TLC, thin layer chromatography; TOPA, 3,4,5-trihydroxyphenylalanine; UV/vis, ultraviolet/visible spectroscopy; XAS, X-ray absorption spectroscopy.

S0006-2960(95)02151-9 CCC: $12.00

Chart 1

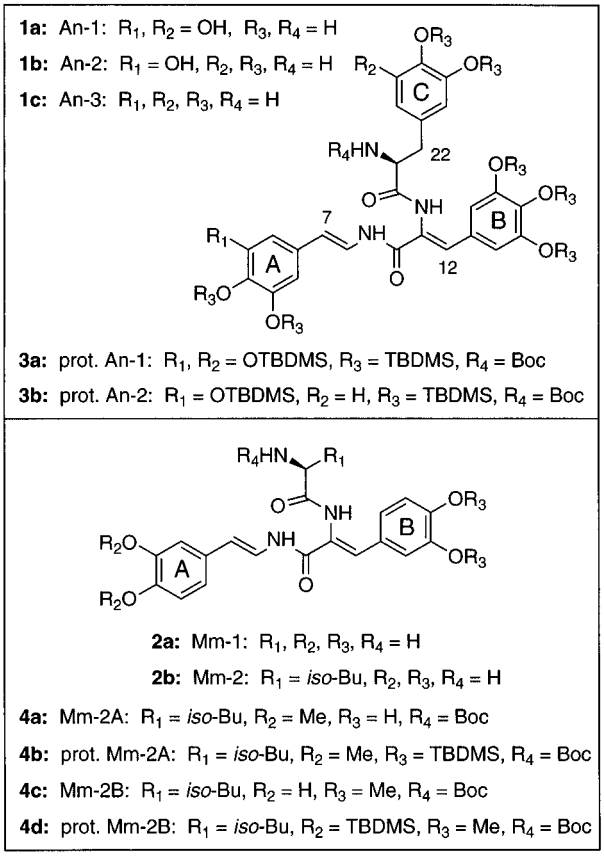

the reduction of V^V or $2V^{IV}$ to the V^{III} state. Such extension of π-conjugation was observed in pH 6.7 media for the tyrosinase oxidation of *N*-acetyl-DOPA ethyl ester, an analog of the C-ring peptide of An-1 **1a** (Taylor et al., 1991). This hypothetical driving force does not exist for Mm-type tunichromes **2** of Fe-accumulating tunicates and may be pivotal to the preference for V-accumulation versus Fe-accumulation.

Other candidates for the native reducing agent of vanadium ions are biogenic thiols. Sulfur K-edge X-ray absorption spectroscopy (XAS) of *A. ceratodes* whole blood cells found high concentrations of endogenous sulfur compounds, including sulfate, alkyl sulfonates, and noncystinyl disulfides (Frank et al., 1987, 1994). In model studies of V^{III} ions in aqueous sulfuric acid, line widths for sulfate in K-edge XAS spectra correlated with pH and V^{III} concentration. Analogously, sulfate line widths in the sulfur K-edge XAS spectra of tunicate blood cells were consistent with a direct interaction between endocytic sulfate and V^{III} ions. This suggests that endogenous thiols (2 mol equiv) may react with V^V to produce V^{III} and a disulfide (which could be further oxidized to alkyl sulfonates or sulfate). Glutathione (GSH), a ubiquitous biogenic thiol (Kosower, 1976), was found to reduce V^V to V^{IV} in human erythrocytes (Macara et al., 1980) and to complex $V^{IV}O$ ions in rat adipocytes (Degani et al., 1981). We were interested in any V^{III} products generated by glutathione under *anaerobic* conditions or by NADPH, dithiothreitol (DTT), or V^{IV}−tunichrome complexes treated with H_2S anaerobically. The relevant reduction potentials $E^{o\prime}$ at pH 7 are (volts vs NHE): −0.23 V for GSSG/2GSH, −0.24 V for S(rhombic)/H_2S, and −0.32 V for $NADP^+$/NADPH (Fasman, 1975), and −0.33 V for DTT disulfide/DTT (Budvari, 1989). For comparison, the reduction potential $E^{o\prime}$ at pH 7 for the V^{IV}/V^{III} couple is calculated to be −0.49 V (Rubinson, 1981), indicating that the thiols and NADPH should not generate V^{III} at pH 7. However, the standard reduction potential E^o for V^{IV}/V^{III} (0.337 V) is higher than E^o for S(rhombic)/H_2S (0.14 V; Fasman, 1975); therefore, the thiols and NADPH may generate V^{III} from V^{IV} or V^V ions under acidic conditions. An alternative hypothesis for the formation of V^{III} in blood cells is that under conditions of anoxia, V^V or $2V^{IV}$ ions substitute for oxygen as the final two-electron acceptor in mitochondria (Smith, 1989). An intriguing new hypothesis is that V^{III} formation is coupled to the electrochemistry of a vacuolar H^+-ATPase identified by immunofluorescence microscopy (Uyama et al., 1994).

To address the question of V^{III} formation in test reactions *in vitro*, we adapted a colorimetric V^{III} assay to analyze air-sensitive, microscale reactions. The assay successfully determined that reactions between Mm-1 **2a** and V^V or V^{IV} ions in pH 7 or pH 2 buffer did not generate appreciable quantities of V^{III} products (Ryan et al., 1996). In this report, the colorimetric V^{III} assay was used to survey the leading candidates for the native reducing agent of vanadate (V^V) in tunicates: An-type tunichromes from V-accumulating tunicates as well as glutathione, NADPH, and H_2S. One candidate, An-type tunichromes, was further studied using vanadium K-edge X-ray absorption spectroscopy (XAS) to characterize vanadium sites in precipitates from mixtures of An-1 and V^V ions under mildly to moderately basic conditions (pH 8.7 and 11). Hence, the range of conditions studied for tunichrome−vanadium complexation and redox chemistry has been extended to include regimes from pH 2 to 11. We also report significant improvements in the isolation of tunichromes **1** from *A. nigra* blood cells via a protection−isolation−deprotection method.

MATERIALS AND METHODS

Synthetic Mm-1 **2a** was previously prepared in protected form (Kim et al., 1990); An-1 **1a** and An-2 **1b** were obtained via a modification of the protection−isolation−deprotection method (see below). Reagents and organic solvents were of the highest purity available from Aldrich and Sigma,

Scheme 1

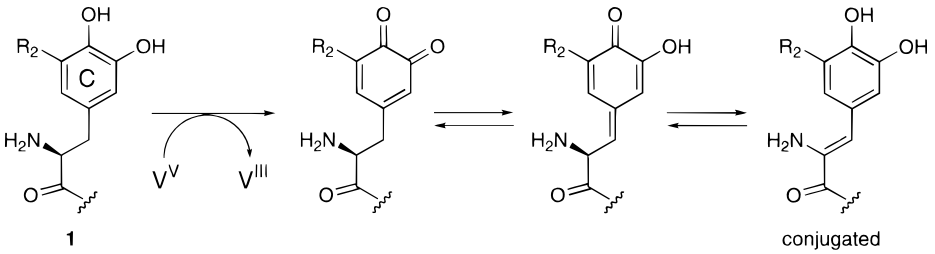

including inorganic solids: VCl_3 (99%), $VOSO_4 \cdot 3H_2O$ (99.99+%), V_2O_5 (99.99%). Water was distilled and deionized. Argon was prepurified grade (99.993%). Aqueous media were deoxygenated in Schlenk flasks by cooling to 4 °C and alternately evacuating (ca. 0.1 torr) and filling with Ar (12×). Organic media were similarly deoxygenated, but cooled to −78 °C. *All reactions were strictly carried out under Ar using airless techniques.* Additions were made via syringe equipped with custom 26- or 24-gauge, 10-inch needles (Hamilton); transfers were made via cannula. UV/vis spectra were recorded on a Perkin-Elmer Model 320 spectrophotometer with background correction.

Isolation of An-1 and An-2. All steps through TBDMS protection were carried out under Ar. The procedure of Kim et al. (1991) was followed with the following modifications. Approximately 500 animals were collected in May, 1993, from Key Biscayne (contact: Dr. Craig Young, Harbor Branch Oceanographic Institute, Ft. Pierce, FL). Blood was withdrawn using 3-mL disposable syringes with 22-gauge needles and was pooled in 50-mL plastic centrifuge tubes sealed with septa under Ar. The crude blood cell pellets were frozen in liquid N_2, lyophilized without thawing, combined (5.4308 g, yellow powder), and ground with anhydrous Na_2SO_4 (5.4 g). For the TBDMS protection step, three solvent systems were screened in small scale reactions (700 mg of pellet/Na_2SO_4 mixture): (i) CH_2Cl_2, (ii) 35% CH_2Cl_2 in THF, and (iii) 7% CH_2Cl_2 in CH_3CN. Boc protection and preparative TLC (2×) gave isolated yields (**3a**, **3b**): (i) 5.0 mg, 1.2 mg, (ii) 6.1 mg, 4.2 mg, and (iii) 3.5 mg, 2.5 mg. The products were identified by ^{1}H NMR (Horenstein & Nakanishi, 1989; D. Kim, unpublished data). The remainder of the pellet/Na_2SO_4 mixture was treated with TBDMS-Cl (50 g) and imidazole (45 g) in CH_2Cl_2/THF (1:2, 360 mL). After aqueous extraction, TBDMS-OH was evaporated under vacuum using a large trap at −78 °C. The crude product was treated with Boc_2O (13.75 g) in CH_2Cl_2 (150 mL). For half of the crude extract, protected An-1 **3a** and An-2 **3b** were isolated by repeated chromatography on silica gel (EtOAc/hexane elution). The other half was dissolved in ethylacetate (250 mL), cooled to 0 °C, and treated with NH_3 bubbled through the solution (1 h, Teflon needle). Chromatography on silica gel gave additional **3a** and **3b** (0.6685 g, total yield). Free An-1 **1a** and An-2 **1b** were obtained via deprotection as described for Mm-1 (Ryan et al., 1996).

The molar extinction coefficient, ϵ, for protected An-1 **3a** in methanol was determined using a hexane solution of **3a** (0.2423 g, 14.39 μmol) prepared in a 100-mL volumetric flask. For five trials, absorbance at λ_{max} 340-1 nm was measured in methanol (940 μL + 60 μL addition), and ϵ was determined (for two batches of An-1).

Colorimetric Assay for V^{III}. The procedures of Crouthamel et al. (1955) and Zolotavin et al. (1962) were modified for air-sensitive, microscale reactions. Custom-made quartz cuvettes (Wilmad) sealed with 8-mm septum screw caps (Wheaton) were washed with concentrated HCl between trials. To generate a calibration curve for the V^{III} assay, a solution of V^{III} was prepared (Frank et al., 1986) as follows:

$$2VOSO_4 + H_{2(g)} + H_2SO_4 \xrightarrow{10\%\ Pd/C} V_2(SO_4)_3 + H_2O$$

A solution of $VOSO_4 \cdot 3H_2O$ (1.08525 g, 5.00 mmol) in H_2SO_4(aq) pH 1.6 (20 mL) was prepared in a 100-mL, 3-neck flask fit with a thermometer adapter (inlet), a water bubbler outlet, and a septum. H_2 and Ar tanks were connected to a three-way stopcock connected to a disposable pipette passed through the thermometer adapter. Argon was bubbled through the solution (30 min), and then wet-type 10% Pd/C (5 mol % Pd) was introduced. Argon bubbling was continued (20 min), and the three-way stopcock was switched to H_2 for slow bubbling (2.5 days). At completion, the flask was purged with Ar. The reddish brown suspension was transferred via Teflon cannula to an airless, fritted glass funnel and filtered through Celite into a 250-mL, three-neck flask with septa. A deoxygenated solution of H_2SO_4(aq), pH 1.6, was used to quantitatively transfer the filtered solution via cannula to a sealed 100-mL volumetric flask. The 100-mL solution was mixed by Ar bubbling. For storage, the 50 mM V^{III} stock solution was transferred to Schlenk tubes. The amount of residual V^{IV} was 1.3% by EPR analysis with comparison to samples of 0.25, 0.5, and 1.0 mM V^{IV} in 50 mM pH 2 buffer.

For the calibration curve for V^{III} assays, a stock solution of 5.0 mM V^{III} in H_2SO_4(aq) pH 1.6 was prepared by diluting an aliquot of the 50 mM stock solution. Also, a stock solution of 3.0 M NH_4SCN in acetone (HPLC grade) was prepared in a volumetric flask then degassed and stored in a Schlenk tube in the dark. (This solution becomes orange reversibly with light exposure. Over a few days, the solution becomes yellow; therefore, fresh solutions were prepared weekly.) To a custom cuvette, concentrated HCl (80 μL) was added via syringe (Teflon needle and syringe Luer hub) to an open cuvette. Water was added so that the total volume would be 400 μL after V^{III} addition. The cuvette was sealed with a septum cap and connected via 23-gauge needle to a vacuum/Ar line. The aqueous HCl in the cuvette was deoxygenated by alternately evacuating and filling with Ar (12×). An aliquot of the 5 mM V^{III} solution (10, 20, or 30 μL) was added followed by an aliquot of 3.0 M NH_4SCN in acetone (600 μL). The solution was mixed by bubbling Ar through a fused silica needle. The needle was made with a piece of deactivated fused silica capillary (J&W Scientific) cemented to a CTFE Luer hub (Hamilton). For each point on the calibration curve, eight trials were averaged; the least-squares fit was linear ($R^2 = 0.999$): $y = (8628\ M^{-1})x + 0.0143$.

For the colorimetric studies, the reaction media were phosphate buffer, pH 7.0 (50 mM), and bisulfate buffer, pH 2.0 (50 mM). Stock solutions of reactants were prepared in volumetric flasks and stored in Schlenk tubes: (i) 5.0 mM V^{IV} in 10 mM bisulfate buffer, pH 2.0, (ii) 5.0 mM V^{V} in 10 mM carbonate buffer, pH 10.0 (V_2O_5 was boiled to dissolve), (iii) 5.0 mM V^{III} in H_2SO_4(aq), pH 1.6, (iv) 5.0 mM $NaIO_4$(aq), and (v) 100 mM DTT(aq) (refrigerated). Stock solutions of ca. 0.5 mM An-1 and ca. 0.5 mM Mm-1 (cf. Ryan et al., 1996) in 20% aqueous methanol were prepared and stored in Schlenk flasks at −70 °C; solutions were calibrated using the ϵ value in methanol (Mm-1: 336−340 nm, 32 500 M^{-1} cm^{-1}; An-1: 336−40 nm, 30 000 M^{-1} cm^{-1}).

Reactions between tunichrome and V^{V} or V^{IV} ions were conducted in acid-washed 10-mL flasks sealed with septa. Care was taken to avoid scraping metal needles inside the flasks. A reaction mixture consisted of V^{V} or V^{IV} (10, 20, or 40 μL) added to an aliquot of tunichrome stock solution (up to 215 μL) in pH 2 or pH 7 buffer (20, 40, or 80 μL,

respectively). A parallel control was prepared using 10 mM pH 10 buffer instead of V^V solution or 10 mM pH 2 buffer instead of V^{IV} solution. The colorimetric reagents were prepared, either before a short reaction (ca. 20 min) or during a long reaction (ca. 1.5 h), in two custom cuvettes as follows. Concentrated HCl (80 μL) and water (appropriate volume to give a total volume of 1 mL after final mixing) were added to two open cuvettes. The cuvettes were sealed and deoxygenated as above. An aliquot (600 μL) of 3.0 M NH_4-SCN in acetone was added to both cuvettes with minimal mixing. After the specified reaction time, the aqueous HCl at the bottom of the cuvettes was transferred to the reaction mixture or control using a fused silica cannula cut from 0.53-mm deactivated tubing (J&W Scientific). The mixtures in the 10-mL flasks were transferred back to the cuvettes and mixed by brief Ar bubbling. In some cases, additional water was added to replace evaporated methanol (cuvettes were calibrated for 1 mL total volume). In a third matched cuvette, the reference for the product mixture and control was prepared: 600 μL of 3.0 M NH_4SCN (in acetone) plus 400 μL of water.

UV/vis spectra were acquired immediately after mixing to avoid interference from a strong red peak (λ_{max} 472 nm) produced by air slowly entering through the punctured septa. To subtract unreacted tunichrome absorption from the product mixture spectrum, a percentage of the control spectrum was subtracted so that the baseline in the visible region (> ca. 370 nm) was flat. Peaks found in the 395−400 nm region were considered V^{III} product if no interfering peaks were found in controls. In some cases, these peaks overlapped with low levels of the red species. The overlapped absorbance of the red species at the 395−400 nm V^{III} peak was approximated as being equal to the nonoverlapped absorbance at 544−549 nm on the opposite side of the symmetrical red peak (λ_{max} 472 nm). The corrected absorbance at 395−400 nm gave the V^{III} concentration from the calibration curve. Additional reactions between An-1 and V^{IV} or V^V were placed under H_2S in a balloon (additions/transfers were made under Ar). Colorimetric studies of DTT instead of tunichrome were conducted as above. Studies of glutathione and NADPH were conducted similarly (Grant, 1994).

X-ray Absorption Spectroscopic Studies. Tunichrome−vanadium complexes were prepared at Columbia University. XAS data were recorded at the Stanford Synchrotron Radiation Laboratory (SSRL). The first sample (V/An-1,2) was prepared by addition of V^V(aq) (0.88 mol equiv) to a solution of An-1 and An-2 (3:2 mixture) in methanol. The V^V solution in NaOH(aq) was pH 11.0. (Buffers were avoided to limit the possible ligands.) Upon addition of V^V, a greenish black precipitate formed immediately. Another sample (V/An-1) was prepared, after sufficient quantities of isolated An-1 became available, by similar addition of V^V(aq) (0.80 mol equiv) to a solution of An-1 in methanol. This V^V solution in NaOH(aq) was pH 8.7, and no precipitate formed upon V^V addition. However, a precipitate was induced by evaporating most of the methanol under vacuum. In both sample preparations, the supernatants were faintly colored suggesting that precipitation of the product mixtures had proceeded nearly to completion.

Preparation of the V/An-1 sample is described in detail. Protected An-1 **3a** (100 mg, 59.4 μmol) was deprotected, and the purity of the product (An-1 **1a**) was acceptable according to ^{1}H NMR analysis (Horenstein & Nakanishi, 1989). Free An-1 was transferred in methanol to a sealed 100-mL volumetric flask, and the concentration of the 100-mL solution was calibrated spectrophotometrically (334−336 nm, 30 000 M^{-1} cm^{-1}) for five aliquots (60 μL) in methanol (940 μL) under Ar. The calibrated concentration gives the overall yield for the deprotection of An-1 (41.6 μmol, 70%). For the addition of V^V to the An-1 solution, a 5 mM V^V solution was prepared by sonicating and boiling V_2O_5 (22.74 mg, 0.125 mmol) in NaOH(aq) pH 10 in a nearly full 50-mL volumetric flask while conc. NaOH(aq) was added dropwise until fully dissolved. The pH of the colorless, 50-mL V^V solution was pH 8.7 (stored in a Schlenk flask). The An-1 solution (ca. 100 mL) was transferred to a 250-mL Schlenk flask, cooled to 0 °C, and treated with 5 mM V^V (6.65 mL, 0.80 mol equiv) by rapid dropwise addition with swirling. After ca. 2 h, a precipitate was induced from the opaque, black solution by evaporating most of the methanol under vacuum using a large trap at −78 °C; a greenish black precipitate formed in the aqueous residue (ca. 15 mL). (Sonication loosened the solid from the flask.) The Schlenk flask was taken into a "wet" glove box (Vacuum Atmospheres Co.) for aqueous samples and opened under prepurified N_2 [the O_2 indicator was equal volumes of 0.7 M catechol(aq) and 2 N NaOH(aq) mixed in the box; colorless solutions indicated inert atmosphere]. The slurry was transferred (rinsing with supernatant) to a 15-mL plastic centrifuge tube and spun in a clinical centrifuge at 1750*g* (20 min) in the glove box. The solid pellet in the tube was placed in a lyophilizer jar connected via rubber tubing to a wide-bore stopcock. The sealed jar was taken from the glove box, placed under Ar, shell frozen in dry ice/acetone bath, and connected to lyophilizer vacuum. After lyophilization overnight, the sealed jar was opened under N_2 in a "dry" glove box. The sample was transported in a Schlenk tube (by D.R.) to Stanford University.

X-ray absorption spectroscopic data for the V/An-1,2 sample were obtained on SSRL wiggler beam line 7-3, under dedicated operating conditions of 3 GeV, a ring current of ∼65 mA, and a wiggler field of 18 kG. Data for the V/An-1 sample were collected on the same SSRL beamline, under similar operating conditions, except that the ring current was ∼45 mA. The X-ray beam was energy resolved using a Si-[220] double crystal monochromator and detuned 50% at 6336 eV (to minimize harmonic contamination). Transmission data were obtained using nitrogen-filled ionization detectors. Vanadium foil calibration data were collected concurrently with the experimental data. Each V/An sample (ca. 20 mg) was prepared by finely grinding the solid sample with boron nitride and then densely and uniformly packing into a 0.5 mm path-length aluminum sample holder, covered with 0.0015 inch kapton windows. Data were collected at 10 K, using an Oxford Instruments CF1208 continuous flow liquid helium cryostat.

Vanadium K-edge XAS data were calibrated relative to the first inflection point on the rising edge of vanadium metal foil, assigned to 5464.0 eV. Reproducibility of X-ray spectra from time-to-time was 0.1−0.2 eV, and spectrometer resolution was about 1 eV. Each raw data scan was corrected for background by fitting a smooth polynomial to the pre-edge region of the spectrum and subtracting the polynomial from the entire spectrum. A polynomial spline was then fit to the data above the edge (Cramer & Hodgson, 1979), and

the total edge-jump intensity was normalized to an absorption of 1.0. The data for the V/An-1,2 sample were the result of nine scans averaged, and the V/An-1 sample data were the average of two scans. Because of a small amount of chromium impurity in the samples, the useful vanadium EXAFS data extended only to about 5990 eV, equivalent to about 10.5 $Å^{-1}$ in *k*-space. This chromium impurity was present in both V/An samples, despite the use of low-chromium vanadate (20 ppm Cr).

Vanadium K-edge XAS spectra of the V/An-1 and V/An-1,2 samples were fit using the nonlinear least-squares fitting program DATFIT4, written by and obtained from Dr. Graham George, Stanford Synchrotron Radiation Laboratory. Each trial to fit a V/An spectrum was made using a selection of XAS spectra of candidate model complexes. The candidate model complexes included: K_3V^{III}(catecholate)$_3$, $(Et_3NH)_2V^{IV}$(catecholate)$_3$, $K_2V^{IV}O$(catecholate)$_2$, $V^{IV}O$(acac)$_2$, $(NH_4)_3V^{V}O_2$(oxalate)$_2$, $NH_4[V^{V}O_2(edtaH_2)]$, $HOV^{V}O$-(8-hydroxyquinoline)$_2$, $V^{V}O$(pivalate)$_3$, and $Na_3V^{V}O_4$. A total of 48 trial fits gave the final fit for V/An-1, and 86 trial fits gave the final fit for V/An-1,2. Acquisition of the V^{III} and V^{IV} model spectra is described elsewhere (Frank et al., 1995). The XAS spectra of the V^{V} model compounds were obtained using solid complexes ground with BN, at 10 K on SSRL wiggler beamline 7−3 under dedicated operating conditions, as noted above for the V/An samples, and were kindly provided by Dr. Ulrich Kuesthardt.

The acceptability of the fits was judged by four different criteria: (1) The relative minimization of error between each fit and the data was assessed, as reflected by the goodness-of-fit parameter *F* (the chi-square test; Press et al., 1992). For fits which differed by small amounts in *F*, detailed visual comparisons of each fit with the data were made over short sections of the pre-edge and edge regions (e.g., 5462−5472, 5472−5485, and 5485−5500 eV). The *F* values of the final fits were ca. 0.9×10^{-4}.

(2) Numerical isolation of the unfit residuals, i.e., the difference between the final fit and the experimental spectrum, revealed only nonsystematic intensity (± 2% of the normalized total edge-jump intensity of a V/An spectrum) about the zero intensity baseline.

(3) The second derivatives of the final fits were required to reproduce the salient portions of the second derivatives of the respective V/An spectra. Success in this criterion is a good indication that the inflections in the actual data are adequately reproduced by the fit to the data. Since the shape of a K-edge XAS spectrum constitutes a spectroscopic fingerprint reflecting all components of a sample, any conclusions regarding the individual components are justified only if all salient features of the XAS data are accurately reproduced by the fit composed of model spectra.

(4) For each ratioed model spectrum (or component) of a final fit, the ratioed model spectrum was compared with the particular portion of the V/An spectrum which was fit by that model spectrum. To reveal this portion of a V/An spectrum, an XAS difference spectrum was constructed from the V/An data by subtracting all ratioed components of the fit except the model component of interest. In general, if an experimental spectrum X was fit by model spectra A, B, and C (e.g., 0.1A + 0.4B + 0.5C), then the part of X which was fit by C, for example, could be extracted as $C_x = [X - (0.1A + 0.4B)]$. The resulting XAS difference spectrum (C_x), which retains all of the unfit residuals, was then visually compared with the ratioed XAS spectrum of model C. If the C_x part of X matched ratioed spectrum C, i.e., if the energy positions and shapes of the XAS spectra of C and C_x were similar, then the unfit residuals were not significant relative to fit component C, and experimental spectrum X was considered to have a spectral component which was well modeled by C. Conversely, if the C_x part of X did not match ratioed spectrum C, then either the intensity of the unfit residuals was significant relative to fit component C, or fit component C was not a good model candidate. In either case, one must rely on the other criteria (1−3 above) to evaluate the acceptability of spectrum C in the fit. Indeed, for the ≤10% components of the final fits (Table 3), the individual difference spectra (analogous to C_x) were not well matched to the corresponding ratioed model spectra, principally because the unfit residuals accounted for ≥20% of the total intensity of each difference spectrum (cf. criterion 2 above). For these low-percentage fit components, however, criteria 1−3 (above) were fully satisfied.

For the K-edge XAS spectra of the V/An-1 and V/An-1,2 samples, the final fits report the percentage of the total edge-jump intensity of each V/An spectrum which was fit by a given model spectrum. Since the goodness-of-fit parameter *F* includes the sum of the square of the residuals, the percentages of the model spectra constituting a fit need not total precisely 100% at minimum *F*. The final fits represented 100 ± 2% of the V/An spectra. In order to facilitate direct comparisons among the fit components, the percentages obtained for a final fit were normalized to total 100.0%. The normalized values are given in Table 3.

The limits of precision of the final fits were evaluated by constructing test XAS spectra consisting of a ratioed sum of selected model XAS spectra of, e.g., 60% $(Et_3NH)_2V^{IV}$-(cat)$_3$ + 20% $V^{IV}O$(acac)$_2$ + 10% K_3V^{III}(cat)$_3$ + 10% $V^{V}O$-(pivalate)$_3$. The value of *F* was monitored in trial fits to the test XAS spectra, carried out by systematically varying the number and identity of model spectra used to fit a given test spectrum. From the systematic fits to the test spectra, the limits of precision at the level of *F* obtained in the final fits to the V/An spectra (ca. 0.9×10^{-4}) were estimated to be 60 ± 6% for a component constituting about 60% of the sample, 20 ± 4% for a 20% component, and 10 ± 5% for a 10% component.

RESULTS AND DISCUSSION

To explore the tunichrome−vanadium redox chemistry of An-1, we isolated An-type tunichromes **1** from ca. 500 living specimens of *A. nigra*. An improved protection−isolation−deprotection method was used for the isolation. The method is quite preservative, strictly anaerobic, and should not cause artifact formation (cf. Ryan et al., 1996). Two significant improvements were made as follows. For the initial TBDMS-Cl/imidazole protection reaction, three solvent systems were screened (CH_2Cl_2, 35% CH_2Cl_2 in THF, and 7% CH_2Cl_2 in CH_3CN) as the original system (CH_2Cl_2) does not dissolve imidazole and tunichromes. In the comparative study, 35% CH_2Cl_2 in THF gave the highest yields of protected An-1 **3a** and An-2 **3b**. The typical solvent for TBDMS-Cl/imidazole protection of phenols is DMF; however, this combination formylated the free amino group of tunichromes (cf. Djuric, 1984). The second improvement was introduced following the Boc_2O protection reaction.

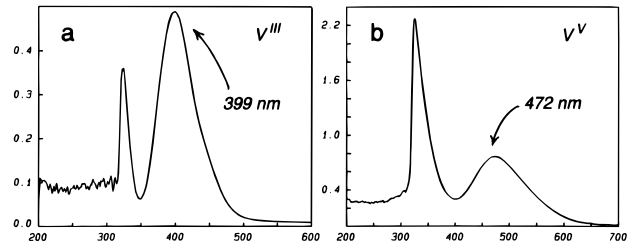

FIGURE 1: (a) *V^{III}:* Absorbance vs wavelength (nm) for 50 μM V^{III} in 1.8 M NH_4SCN/1 M HCl in 6:4 acetone/water. (b) *V^{V}:* Absorbance vs wavelength (nm) for 50 μM V^{V} in 1.8 M NH_4SCN/1 M HCl in 6:4 acetone/water.

Excess Boc_2O is not hydrolyzed during aqueous extraction and is difficult to separate from protected An-1 and An-2 by silica gel chromatography (Boc_2O appears blue by vanillin staining). By bubbling NH_3 through a cooled solution of the crude product, aminolysis of Boc_2O gives polar by-products which are readily separated. From the ca. 500 specimens of *A. nigra*, sufficient quantities of protected An-1 **3a** and An-2 **3b** were obtained; however, no protected An-3 was found (cf. Oltz et al., 1988; Kim et al., 1991). The molar extinction coefficient, ϵ (M^{-1} cm^{-1}), for protected An-1 was determined in methanol (340−341 nm, 30 100 ± 300). Based on the observation that protected and deprotected tunichrome have nearly the same ϵ value in a mutual solvent (Ryan et al., 1996), the ϵ value for protected An-1 in methanol was used for deprotected An-1 **1a** in methanol. For a large-scale deprotection of An-1 (XAS studies below), an ϵ of 30 000 gives a reasonable overall yield of 70%, whereas the previously reported ϵ for An-1 (19 600 M^{-1} cm^{-1}; Bruening et al., 1985) gives an impossible yield of 107%.

Colorimetric Assay for V^{III}. A colorimetric assay for V^{III} using ammonium thiocyanate reagent (1.8 M NH_4SCN/1 M HCl in 6:4 acetone/water) was adapted for air-sensitive, microscale reactions from literature procedures (Crouthamel et al., 1955; Zolotavin et al., 1962). The yellow $V^{III}(SCN)_6$ complex absorbs maximally at 396−399 nm (lit. 11 700 M^{-1} cm^{-1}) (Figure 1a; spectra are essentially cut off below 330 nm due to the saturated UV absorption of acetone in sample and reference cuvettes). As we confirmed, the V^{IV} complex, $V^{IV}O(SCN)_2$, has a much lower molar absorptivity (lit. ϵ 435 M^{-1} cm^{-1} at 760 nm) and does not interfere with V^{III} detection. Thiocyanate is oxidized by V^{V}, as well as by $NaIO_4$, metal contaminants from needles, and V^{IV} exposed to air producing a strong red band at 472 nm (Figure 1b). Low levels of this band do not interfere with the V^{III} assay.

A calibration curve was generated for the V^{III} assay at concentrations of V^{III} (50, 100, and 150 μM) giving optimal absorbances (0.463 ± 3.3%, 0.886 ± 2.9%, and 1.297 ± 1.8%, respectively). The calibration curve obeyed Beer's Law—the least-squares fit was linear ($R^2 = 0.999$) and gave a molar extinction coefficient of 8630 M^{-1} cm^{-1} at 396−399 nm. The detection limit for the V^{III} assay at a 2:1 signal-to-noise ratio was ca. 2 μM V^{III}. Reactions between tunichrome and V^{V} or V^{IV} ions at assay concentrations involved modest quantities of tunichrome (e.g., 50 μM in a 1-mL cuvette). The acidic conditions of the assay (1 N HCl) are desirable because, at pH ≤2, tunichromes will not interfere competitively with thiocyanate complexation of V^{III}. This is based on the observation that tunichrome Mm-1 **2a** does not form stable complexes of vanadium ions in pH 2 buffer (Ryan et al., 1996). Similarly, catechol does not form stable complexes of V^{IV} at pH < 2.3 (Shnaiderman et al., 1972; Buglyò et al., 1993).

Table 1: Colorimetric Assay for V^{III} in An-1 Reactions

reactant	[V] (μM)[a]	buffer	time
V^{IV} (14.7 equiv)	400	pH 2	20 min
V^{IV} (14.7 equiv)	400	pH 2	1.5 h
V^{IV} (0.33 equiv)	50	pH 2	1.5 h
V^{V} (7.4 equiv)	200	pH 2	1.5 h
V^{V} (1.8 equiv)	50	pH 2	1.5 h
V^{V} (0.33 equiv)	50	pH 2	1.5 h
V^{IV} (14.7 equiv)	400	pH 7	20 min
V^{IV} (14.7 equiv)	400	pH 7	1.5 h
V^{IV} (7.4 equiv)	200	pH 7	20 min
V^{IV} (7.4 equiv)	200	pH 7	1.5 h
V^{IV} (0.33 equiv)	50	pH 7	20 min
V^{IV} (0.33 equiv)	50	pH 7	1.5 h
V^{V} (7.4 equiv)	200	pH 7	20 min
V^{V} (7.4 equiv)	200	pH 7	1.5 h
V^{V} (1.8 equiv)	50	pH 7	20 min
V^{V} (1.8 equiv)	50	pH 7	1.5 h
V^{V} (0.33 equiv)	50	pH 7	20 min
V^{V} (0.33 equiv)	50	pH 7	1.5 h

[a] Concentration of total vanadium in the colorimetric sample.

Colorimetric V^{III} assays were conducted for anaerobic reactions between An-1 and V^{V} or V^{IV} ions in methanolic aqueous buffer (pH 2 or 7) under various conditions *in vitro* (Table 1). For the V^{IV} reactions and for the V^{V} reactions in pH 2 buffer, no V^{III} products were found. [Positive control assays were produced by injecting an aliquot (1 mol equiv) of V^{III} stock solution into the completely assayed product mixtures.] However, for the V^{V} reactions in pH 7 buffer, a small peak appeared in the 400−420 nm region for all reactions. This peak cannot be assigned as due to V^{III}, however, because control reactions using $NaIO_4$ oxidant instead of V^{V} reactant generated a similar peak without any vanadium present. To clearly demonstrate that the peak for the $NaIO_4$ controls was due to oxidized An-1, the same amount of An-1 (28 pmol) was fully oxidized with $NaIO_4$ (4 mol equiv) in pH 7 buffer (1 h; 1 mL total volume) without addition of the colorimetric reagents. As in the colorimetric studies, unreacted An-1 absorption was subtracted to give a flat baseline above ca. 370 nm. Thus, the oxidized An-1 product mixture showed a peak of expected intensity at 402 nm, close to the λ_{max} of $V^{III}(SCN)_6$ (396−399 nm). The 402 nm peak was produced in pH 7 buffer selectively and not under parallel conditions in pH 2 buffer. The red-shifted peak at 402 nm for oxidized An-1 may arise from completion of π-conjugation in An-1 via oxidation of the C ring (as in Scheme 1; Taylor et al., 1991). Such a peak was not found under similar conditions for Mm-1 **2a**, which lacks a C ring (Ryan et al., 1996).

The assay results for An-1 clearly show that reactions with V^{IV} (all conditions) or with V^{V} in pH 2 buffer did not generate detectable quantities of V^{III} products under the conditions tested (Table 1). However, for reactions between An-1 and V^{V} in pH 7 buffer (Table 1), low levels of V^{III} products could not be ruled out because of the interfering peak (<15 μM V^{III} was possible).

As a continuation of the survey of biogenic reducing agents which may generate V^{III} in tunicates, the colorimetric V^{III} assay was used to assay anaerobic reactions between V^{V} or V^{IV} ions and glutathione (biogenic), NADPH (biogenic), DTT, or $Na_2S_2O_4$ (positive control) under various conditions

Table 2: Colorimetric Assay for V^{III} in Thiol Reactions

reactants	[V] (μM)[a]	pH	time (h)
V^{IV} + GSH (100 equiv)	250	0	1
V^{IV} + GSH (100 equiv)	375	1	12
V^{IV} + GSH (100 equiv)	500	2	12
V^{IV} + GSH (100 equiv)	500	3	12
V^{IV} + GSH (8 equiv), GR, NADPH[b]	250	7.6	2
V^{V} + GSH (100 equiv)	250	0	1
V^{V} + GSH (100 equiv)	375	1	12
V^{V} + GSH (100 equiv)	500	2	12
V^{V} + GSH (100 equiv)	500	3	12
V^{V} + GSH (2 equiv)	56 000	7	12
V^{V} + GSH (8 equiv), GR, NADPH[b]	250	7.6	2
V^{V} + GSH (8 equiv), GR, NADPH[b]	250	7.6	12
V^{IV} + NADPH (50 equiv)	345	1	1
V^{V} + NADPH (50 equiv)	345	1	1
V^{V} + NADPH (50 equiv)	345	1	12
V^{IV} + $Na_2S_2O_4$ (100 equiv)	375	1	12
V^{V} + $Na_2S_2O_4$ (100 equiv)	375	1	12
V^{IV} + DTT (100 equiv)	50	2	1
V^{IV} + DTT (100 equiv)	50	7	1
V^{V} + DTT (100 equiv)	50	2	1
V^{V} + DTT (100 equiv)	50	7	1
V^{IV} + An-1 (3 equiv) under H_2S	50	2	1
V^{IV} + An-1 (3 equiv) under H_2S	50	7	1
V^{V} + An-1 (3 equiv) under H_2S	50	2	1
V^{V} + An-1 (3 equiv) under H_2S	50	7	1

[a] Concentration of total vanadium in the colorimetric sample. [b] Incubated in the presence of glutathione reductase (GR) and NADPH.

in vitro (Table 2). Also, reactions between An-1 and V^{V} or V^{IV} ions were conducted under H_2S (biogenic). Large excesses of the reducing agents were screened to favor the formation of V^{III}. Glutathione was sometimes used in the presence of glutathione reductase (GR) and NADPH cofactor. Of the various conditions screened (Table 2), only sodium dithionite reactions gave a positive assay for V^{III} products ($E^{o} = -1.12$ V for $SO_3^{2-}/S_2O_4^{2-}$; Lide, 1993). For the other conditions, positive control assays were produced by injecting an aliquot (1 mol equiv) of V^{III} stock solution into the completely assayed product mixtures. Therefore, we can conclude that glutathione, NADPH, DTT, and H_2S did not generate detectable quantities of V^{III} products under the conditions tested (Table 2).

The combined results of colorimetric V^{III} assays for biogenic reducing agents found that neither Mm-1 (Ryan et al., 1996), An-1, glutathione, NADPH, DTT, nor H_2S generated appreciable quantities of V^{III} products under the conditions tested. However, low levels of V^{III} products could not be ruled out for reactions between An-1 and V^{V} ions in pH 7 buffer. In mildly to moderately basic media, solutions of An-1 and V^{V} ions produced a greenish black precipitate upon mixing as previously described and partially characterized by Oltz et al. (1988). The precipitate was prepared and isolated under anaerobic conditions (see below) and exhibited the same solubility and UV/vis characteristics reported by Oltz et al. The precipitate dissolved only in aqueous acid, which dissociates vanadium(catecholate)-type complexes. Additionally, we obtained a solid-state EPR spectrum and a diffuse reflectance FT-IR spectrum of the precipitate under Ar (data not shown), but the features of both spectra were broad and could not be assigned. In attempts to obtain a solid-state resonance Raman spectrum at 77 K and an electrospray mass spectrum of the precipitate dissolved in aqueous acid, the samples decomposed during analysis. Therefore, the crude precipitate was analyzed using vanadium K-edge X-ray absorption spectroscopy (XAS), under anaerobic conditions, to characterize the ligand environments and oxidation states of vanadium sites in the precipitated product mixture.

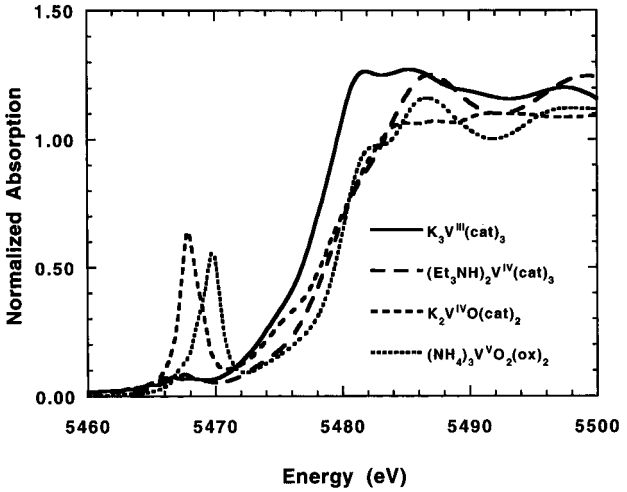

FIGURE 2: X-ray absorption K-edge spectra of selected vanadium model complexes. These spectra are identified on the figure. The different edge positions correlate with changes in metal oxidation state and ligand identity. The symmetry of a metal−ligand site affects the strength of the K-edge transition and thus the shape of the edge. The features near 5468−5469 eV reflect 1s → LUMO (V═O) transitions and are quite intense due to lowered site symmetry and the d−p orbital mixing in metal−oxo bonds.

X-ray Absorption Spectroscopic Studies. Structural information about transition metal sites in amorphous solids, biological samples, and homogeneous solutions can be obtained using X-ray absorption spectroscopy. Vanadium K-edge XAS was found to be the most suitable technique for characterizing vanadium sites in the greenish black precipitates isolated from mixtures of V^{V} and An-1 or a 3:2 An-1/An-2 mixture, in mildly to moderately basic media (pH 8.7 and 11, respectively). The precipitated V/An-1 and V/An-1,2 samples were prepared and analyzed under rigorously anaerobic conditions. For comparison to the V/An samples, catecholate complexes of V^{IV} and V^{III} [i.e., $K_2V^{IV}O(cat)_2$, $(Et_3NH)_2V^{IV}(cat)_3$, and $K_3V^{III}(cat)_3$] were prepared according to literature methods (Cooper et al., 1982) and were analyzed by vanadium K-edge XAS (Frank et al., 1995).

The XAS technique is element-selective and can yield information regarding oxidation state, ligation environment, and symmetry of the absorbing element by analysis of the edge region of the spectrum. From analysis of the extended X-ray absorption fine structure (EXAFS), one can determine the identity, number, and distance of the neighboring atoms (e.g., the ligating atoms of a transition metal complex). For transition metal complexes, K-edge XAS spectra involve energy-dependent electronic transitions from the 1s core of the absorbing metal ion to the valence orbitals, which include contributions from coordinated ligands. Transitions to higher energy orbitals can also be observed, up to the ionization energy of the metal ion. For a short overview of the method, see Smith et al. (1995).

Characteristics of vanadium K-edge XAS spectra are exemplified by the spectra of catecholate complexes $K_3V^{III}(cat)_3$, $(Et_3NH)_2V^{IV}(cat)_3$, and $K_2V^{IV}O(cat)_2$, and oxalate complex $(NH_4)_3V^{V}O_2(oxalate)_2$ (Figure 2). Obvious and diagnostic spectral features are (i) the variation in edge position with oxidation state and ligand identity, and (ii) the

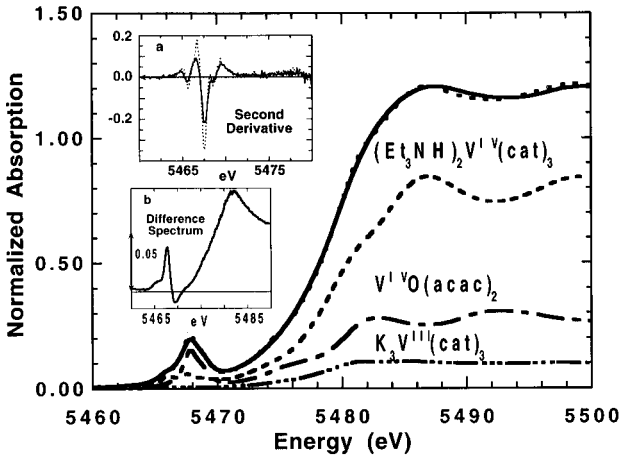

FIGURE 3: X-ray absorption spectra of V/An-1 (—), the fit (- - -) to V/An-1, and the three major components of the fit. These components are identified on the face of the figure and in Table 3. Insets: (a) Second derivative XAS spectra of V/An-1 (—) and the fit (- - -) to V/An-1; (b) V/An-1 minus V/An-1,2 difference spectrum (see text for discussion). The double-headed arrow marks the range between zero and 0.05 intensity units. The negative intensity in the pre-edge region reflects the small V^V═O component in the V/An-1,2 spectrum which is not present in the XAS spectrum of V/An-1. [Note: A plot of the unfit residuals (not shown) showed only nonsystematic intensity (±2% of the normalized total edge-jump intensity of the V/An-1 spectrum) about the zero intensity baseline.]

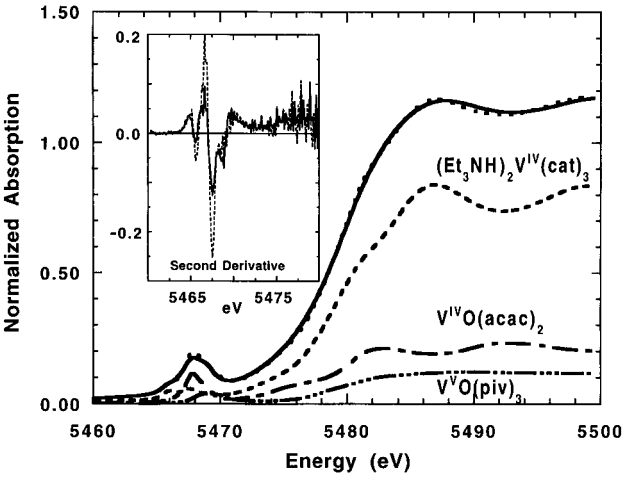

FIGURE 4: X-ray absorption spectra of V/An-1,2 (—), the fit (- - -) to V/An-1,2, and the three major components of the fit. These components are identified on the face of the figure and in Table 3. Inset: Second derivative XAS spectra of V/An-1,2 (—) and the fit (- - -) to V/An-1,2. [Note: A plot of the unfit residuals (not shown) showed only nonsystematic intensity (±2% of the normalized total edge-jump intensity of the V/An-1,2 spectrum) about the zero intensity baseline.]

intense pre-edge features at 5468−5469 eV produced by the vanadium−oxo bond(s) (V═O) of the latter two complexes. Such pre-edge signature features of metal−oxo (M═O) complexes arise from a 1s → LUMO (M═O) transition that gains intensity due to the noncentric ligand field and to d−p orbital mixing in the M═O bond (Ballhausen & Gray, 1962; Kutzler et al., 1981; Penner-Hahn et al., 1986).

The vanadium K-edge spectra of V/An-1 and V/An-1,2 samples are shown in Figures 3 and 4. In order to estimate the types of vanadium complexes which might exist in the V/An samples, we fit the V/An XAS spectra with the K-edge XAS spectra of vanadium model complexes (see Materials and Methods). Vanadium−catecholate complexes are appropriate structural models for tunichrome−vanadium complexes, especially since it was observed by EPR spectroscopy that *N*-Boc protected Mm-1 tunichromes reacted with V^V ions [$NaCO_3$(aq) pH 8.1] in aqueous methanol to generate bis(catecholate)-type $V^{IV}O$ and tris(catecholate)-type V^{IV} complexes (Grant, 1994; Grant et al., 1996). Therefore, a set of candidate vanadium K-edge XAS model spectra was assembled, including spectra of the catecholate complexes $K_3V^{III}(cat)_3$, $K_2V^{IV}O(cat)_2$, and $(Et_3NH)_2V^{IV}(cat)_3$. Vanadium K-edge XAS spectra of various noncatecholate complexes of $V^{IV}O$ and V^VO were also included in the model set to provide pre-edge features of a range of V═O bond motifs. The strong 1s → LUMO (V═O) pre-edge features of V═O complexes have characteristic shapes and energy positions. In the V/An XAS spectra, minor V═O components made significant contributions to the spectra, especially in the pre-edge region near 5468−5469 eV where the intense 1s → LUMO (V═O) transitions dominate. The energy position of a V═O pre-edge feature is dependent on the oxidation state and the ligand environment of the central vanadium ion (Kutzler et al., 1981; Wong et al., 1984) (cf. Figure 2). Because these V═O features are relatively intense in K-edge XAS spectra, they influenced the goodness of fit parameter *F* to a greater degree than might be expected from the proportionate contribution of the relevant spectrum to the fit. Therefore, the intensities and eV positions of the V═O pre-edge features tightly constrained the choice of which oxo-vanadium model spectrum was appropriate to each fit. The XAS spectra of the noncatecholate V═O complexes proved to be useful for modeling the minor V═O components of the V/An spectral data.

Table 3: Fits to the K-edge XAS Spectra of V/An-1 and V/An-1,2 Samples

fit component[a]	V/An-1[b]	V/An-1,2[b]
$K_3V^{III}(catecholate)_3$	9%	1%
$(Et_3NH)_2V^{IV}(catecholate)_3$	63%	69%
$K_2V^{IV}O(catecholate)_2$	2%	0%
$V^{IV}O(acetylacetonate)_2$	23%	20%
$V^VO(pivalate)_3$		11%
$HOV^VO(8\text{-hydroxyquinolinate})_2$	3%	
goodness of fit ($F \times 10^{-4}$)[c]	0.905	0.890
total Vanadium(III)	9%	1%
total Vanadium(IV)	88%	88%
total Vanadium(V)	3%	11%
average vanadium oxidation state	3.9+	4.1+

[a] The fit component is the model compound whose K-edge XAS spectrum was fit to the K-edge XAS spectrum of the V/An-1 or V/An-1,2 sample. The percentage found for a fit component is the percentage of the total edge-jump intensity (normalized to an absorption of 1.0) of the V/An spectrum which was fit by the given model spectrum (normalized also). The total percentage was normalized to 100% (cf. Materials and Methods). [b] Approximate limits of precision are discussed in Materials and Methods. [c] Goodness of fit, *F*, is given by the chi-square test (Press et al., 1992). Perfect fits to test spectra composed of ratioed model spectra yielded $F \cong 0.5 \times 10^{-8}$.

The final results of the fitting experiments are shown in Figures 3 and 4 and listed in Table 3. Since the model complexes do not provide vanadium environments identical to those in V/An complexes, the resultant spectral fits are approximate representations. Inspection of Figures 3 and 4 reveals that the fits successfully reproduced the salient shapes, energy positions, and multiplicities of the original V/An XAS spectra. In judging the acceptability of the fits (see Materials and Methods), the second derivatives of the fits were compared with the second derivatives of the V/An

XAS spectra. The XAS spectrum of a given compound contains a unique set of inflection points at slope changes in the plot. The second derivative is especially sensitive to the inflection points, such that inflections which are hidden to the eye are revealed in the second derivative plot, even in rather featureless regions of a spectrum. The intensity of the second derivative of an absorption peak (in a normalized spectrum) is a measure of the width of that peak. The XAS spectrum for a mixture of compounds has absorption peaks, shoulders, and inflection points that result from the sum of the spectra of the individual components of the mixture. These characteristic spectral features yield a unique second derivative spectrum which serves as a fingerprint for the particular mixture (George et al., 1991; Pickering et al., 1995). Therefore, it is extremely unlikely that the second derivative of an inaccurate fit could precisely conform to the second derivative of the sample spectrum. In our experiments, the second derivatives of the final fits conformed to the energy positions and shapes of the second derivatives of the V/An spectra, even in the detailed pre-edge XAS regions (insets, Figures 3 and 4). This conformity suggests that the fits accurately represent the V/An XAS data. Furthermore, the vanadium sites of the model compounds which constituted the final fits are good spectroscopic models for the vanadium sites in the V/An samples.

The major portions of both V/An XAS spectra were fit by the $(Et_3NH)_2V^{IV}(cat)_3$ model spectrum. To reveal the particular portion of each V/An spectrum which was fit by the $(Et_3NH)_2V^{IV}(cat)_3$ model spectrum, an XAS difference spectrum was constructed from each V/An spectrum by subtracting all ratioed components of the fit except for the $(Et_3NH)_2V^{IV}(cat)_3$ component (see Materials and Methods). The XAS difference spectra so obtained from the V/An-1 and the V/An-1,2 XAS spectra were virtually superimposable, including the weak pre-edge transitions. Both difference spectra strongly resembled the XAS spectrum of authentic $(Et_3NH)_2V^{IV}(cat)_3$, including a close reproduction of the weak 1s → 3d pre-edge features. Therefore, the major component of both V/An product mixtures is most consistently attributed to spectroscopically equivalent, non-oxo V^{IV} complexes that include a tunichrome ligand array similar to that of the V^{IV}−tris(catecholate) model complex.

The $V^{IV}O(acac)_2$ model spectrum also made significant contributions to both of the V/An fits. Although the analogous catecholate complex $K_2V^{IV}O(cat)_2$ is an intuitively superior model for any $V^{IV}O$−tunichrome complexes produced, the V/An spectra were much better fit with the spectrum of $V^{IV}O(acac)_2$, as judged both by the goodness-of-fit parameter, *F*, and by visual inspection. In comparing the XAS spectra of $V^{IV}O(acac)_2$ and $K_2V^{IV}O(cat)_2$ models, both have 1s → LUMO (V^{IV}═O) pre-edge transitions at 5468 eV that are similar in intensity, energy position, and shape. At higher energy, the spectrum of $V^{IV}O(acac)_2$ exhibits two strong transitions at 5482.9 and 5492.7 eV, just above the absorption edge. In contrast, the spectrum of $K_2V^{IV}O(cat)_2$ is essentially flat and featureless above the absorption edge (i.e., at energies > 5484.9 eV). The particular portion of each V/An spectrum which was fit by the spectrum of $V^{IV}O(acac)_2$ was examined by constructing a ratioed XAS difference spectrum (as above). As noted in the previous case, the V/An-1 and V/An-1,2 XAS difference spectra were nearly superimposable, implying spectroscopically equivalent products. Both difference spectra had an overall shape that was quite similar to the XAS spectrum of authentic $V^{IV}O(acac)_2$, including a strong 1s → LUMO (V^{IV}═O) transition at 5467.9 eV, and two strong transitions at 5483 and 5492 eV, above the K-edge maximum. Therefore, $V^{IV}O(acac)_2$ is a reasonable spectroscopic model for a V═O component present in both V/An samples.

The region above the K-edge maximum (or edge jump) is governed by electronic transitions from the 1s orbital to higher energy atomic and molecular orbitals, shape resonances, and multiple scattering transitions (Wong et al., 1984; Benfatto et al., 1986). These transitions are sensitive to the geometry and electronic state of the ligand. It may be that the component of each V/An spectrum fit by the spectrum of $V^{IV}O(acac)_2$ reflects participation of vanadium in delocalized, tunichrome molecular orbitals which are more analogous, in some respects, to molecular orbitals provided by the ligand environment of $V^{IV}O(acac)_2$ than to those of $K_2V^{IV}O(cat)_2$.

Of the three pre-edge features in the second-derivative V/An-1,2 XAS spectrum (inset, Figure 4), that at highest energy (5468.7 eV) probably reflects a V^{V}═O component. This feature appears as a shoulder on the high-eV side of the pre-edge features in the K-edge absorption spectrum and was best fit by the $V^{V}O(pivalate)_3$ model spectrum (cf. Table 3). Although $V^{V}O(pivalate)_3$ is not a catecholate-type complex, its strong V^{V}═O pre-edge feature modeled the pre-edge transition of a possible $V^{V}O$−tunichrome complex in the V/An-1,2 sample. In contrast to the V/An-1,2 spectrum, no significant contribution from V^{V} was needed to fit the XAS spectrum of V/An-1 (Figure 3). Although the best fit to the V/An-1 data included a minor contribution from the $HOV^{V}O(8\text{-hydroxyquinolinate})_2$ model spectrum, the level of this contribution (3%) makes it difficult to impute much meaning to it. Similarly, a minor component (2%) of $K_2V^{IV}O(cat)_2$ fit to the V/An-1 spectrum is too small to interpret. These components most likely reflect unfit residuals in the data but are included in Table 3 for completeness.

Of particular relevance to ascidian biochemistry is the portion of the V/An-1 XAS spectrum fit by a 9% contribution from the $K_3V^{III}(cat)_3$ model spectrum (cf. Figure 3 and Table 3). To examine this V^{III}-like component of the V/An-1 data, an XAS difference spectrum was constructed from the V/An-1 spectrum by subtracting all of the non-V^{III} ratioed fit components (as above). The difference spectrum exhibited a rising edge at 5477.7 eV, consistent with a V^{III} assignment. However, it did not closely resemble the XAS spectrum of authentic $K_3V^{III}(cat)_3$ (rising edge at 5479.5 eV), in contrast to the XAS difference spectra reflecting the portions of the original V/An spectra fit by the $(Et_3NH)_2V^{IV}(cat)_3$ and $V^{IV}O(acac)_2$ model spectra (discussed above). Rather, the difference spectrum appeared to reflect the superposition of the V^{III} edge and all of the unfit residuals present in such a difference spectrum (see Materials and Methods). Examination of the unfit residuals themselves showed nonsystematic intensity, indicating that little of significance remained unfit.

Substantial support for the presence of V^{III} species in the V/An-1 sample was obtained by subtracting the comparable V/An-1,2 spectrum from the V/An-1 spectrum. This XAS difference spectrum (inset b, Figure 3) revealed the low-eV portion of the V/An-1 spectrum which exhibited a rising edge at 5479.5 eV, consistent with a V^{III} assignment. Therefore, the V^{III} edge feature is present primarily in the V/An-1

spectrum and cannot be an unfit residual of any component equally present in both V/An spectra, which in fact were found to have nearly equal levels of the major components (cf. Table 3).

Since any unoxidized An-1 in the V/An-1 sample could have provided a highly electron-donating ligand for some of the V^{IV} ions produced, we considered the possibility that such a V^{IV} complex might have produced the V^{III}-like difference edge feature at 5479.5 eV (Figure 3, inset b). However, existant data relating XAS edge shifts to vanadium oxidation state changes and to ligand effects argue otherwise. For example, a linear correlation of -2.4 ± 0.3 eV edge shift per unit decrease in oxidation state was reported for a series of solid vanadium oxides (Wong et al., 1984). The XAS K-edge jump for $V^{II}(H_2O)_6^{2+}$ was reported to be 4.9 eV lower in energy than that for $V^{III}(H_2O)_6^{3+}$ (Miyanaga et al., 1990). Similarly, the energy difference between the K-edge jumps of $V^{III}(cat)_3^{3-}$ and $V^{IV}(cat)_3^{2-}$ was 4.3 eV (cf. Figure 2), and the difference between those of $V^{III}(H_2O)_6^{3+}$ and $V^{IV}(cat)_3^{2-}$ was 3.4 eV (unpublished results). In general, a K-edge separation of ca. 2.4−4.9 eV corresponds to a unit change in oxidation state for a series of oxygen-ligated vanadium ions. For vanadium complexes of a single oxidation state but with various oxygen-bonded ligands, the range of K-edge energies is much smaller, on the order of 0.2−1.0 eV, depending on the similarities of the ligation spheres (Wong, et al., 1984; unpublished results). The V^{III}-like portion of the V/An-1 sample produced a K-edge feature at 5479.5 eV, 0.9 eV lower in energy than the K-edge of $V^{III}(H_2O)_6^{3+}$, and 4.3 eV lower in energy than the K-edge of the spectrum of the $(Et_3NH)_2V^{IV}(cat)_3$ model. These energy differences are far too large to be attributed to ligand effects only. Therefore the K-edge feature at 5479.5 eV in the V/An-1 spectrum is within the regime of V^{III} oxidation states. Hence, the portion of the V/An-1 sample that produced this low-eV difference feature is most consistently attributed to a minor V^{III} product.

In general, the fits to the V/An spectra indicate that the major redox products in the V/An samples were V^{IV} complexes. The subtle differences between the two V/An samples, especially the percentages of V^{III} and V^{V} products, were most likely due to the different preparative conditions, i.e., initial pH, mole equivalents of V^{V} reactant, concentrations for precipitation, and total time in solution (see Materials and Methods). The conditions necessary for generating V^{III} products may have been achieved during precipitation, as a comparable reaction between pyrogallol and $V^{IV}O(acac)_2$ in anhydrous THF generated a V^{III} complex, apparently by the exclusion or limitation of water (Lee et al., 1988b). By analogy, the process of precipitation could have caused localized exclusions of water that promoted V^{III} product formation in the V/An-1 sample preparation.

Interestingly, in both V/An samples, most of the V^{IV} products lacked an oxo ligand and were similar to the tris(catecholate) model, $(Et_3NH)_2V^{IV}(cat)_3$. The formation of tris(catecholate)-type V^{IV} complexes in aqueous media generally requires a large excess of ligand (Branca et al., 1990), which was not present in the V/An sample preparations. Low temperature EPR studies of reactions between An-1 or Mm-1 and V^{V} ions found that tunichromes produced tris(catecholate)-type V^{IV} complexes in neutral aqueous solution to a greater extent than did catechol (Grant, 1994; Grant et al., 1996). For V^{IV} complexes in the V/An XAS samples, the V^{IV} metal centers were complexed by partially oxidized An-1, presumably at the unoxidized catecholate rings. This presumption is based on results from spectrophotometric studies of Mm-1 under similar conditions (Ryan et al., 1996). Upon treatment with V^{IV} ions, partially oxidized Mm-1 mixtures showed large red-shifts (ca. 40 nm) indicative of V^{IV} complexation, whereas fully oxidized Mm-1 mixtures showed slight red shifts (<5 nm) indicating that only very limited or weak complexation was possible. The XAS finding of predominantly V^{IV}-complexed redox products is consistent with data obtained from EPR studies of An-1 and Mm-1 (Grant, 1994; Grant et al., 1996) and spectrophotometric studies of Mm-1 (Ryan et al., 1996) under similar conditions.

CONCLUSION

Reactions between vanadium ions and biogenic reducing agents of tunicates were studied *in vitro* using spectroscopic methods to probe for complexation and/or redox products. A sensitive colorimetric V^{III} assay was used to survey the leading candidates for the native reducing agent of vanadate in tunicates (i.e., An-type tunichromes, glutathione, NADPH, and H_2S) in reactions with V^{V} or V^{IV} ions under anaerobic, aqueous conditions at acidic or neutral pH. Except for the case of An-1 and V^{V} ions in pH 7 buffer, the assay results for the biogenic reducing agents clearly showed that appreciable quantities of V^{III} products were not generated under the conditions tested. For reactions between An-1 and V^{V} ions in pH 7 buffer, low levels of V^{III} products could not be ruled out because of an interfering peak in the colorimetric assays.

For similar reactions between V^{V} ions and An-1, or an An-1,2 mixture, in mildly to moderately basic media, the product mixtures precipitated as greenish black solids. Vanadium K-edge XAS analyses of the precipitated V/An mixtures showed that the major products were tris(catecholate)-type V^{IV} complexes ($65 \pm 6\%$) and bis(catecholate)-type $V^{IV}O$ complexes ($20 \pm 4\%$). Remarkably, the analogous V^{IV} complexes in the two V/An samples were essentially indistinguishable by K-edge XAS analysis and were produced in nearly the same ratios. XAS analysis of the V/An-1 product mixture also provided evidence of a minor V^{III} component ($9 \pm 5\%$ of total V), notable for possible relevance to tunicate biochemistry.

The XAS observation of predominantly tris(catecholate)-type V^{IV} complexes was unexpected. The formation of V^{IV}−tris(catecholate) complexes in aqueous media generally requires a large excess of ligand (Branca et al., 1990), which was not present in the V/An sample preparations. The combined results of XAS studies (reported herein), spectrophotometric studies (Ryan et al., 1996), and EPR studies (Grant et al., 1996) consistently establish that reactions between tunichromes (Mm-1 or An-1) and V^{V} ions generate predominantly V^{IV}−tunichrome complexes in neutral to moderately basic aqueous media.

The colorimetric results place new limits on hypothetical mechanisms of V^{III} formation *in vivo*. Under the anaerobic, aqueous conditions tested *in vitro*, neither tunichromes (Mm-1 and An-1) nor biogenic thiols (glutathione and H_2S) proved capable of producing the high concentrations of V^{III} present in tunicate blood cells. However, tunichromes may

generate high levels of V^{III} in a cellular environment by exclusion or limitation of water, analogous to the reduction of $V^{IV}O(acac)_2$ by pyrogallol in anhydrous THF which yielded a V^{III} dimer (Lee et al., 1988b). Reduction potentials of transition metal ions are often higher in hydrophobic binding sites. Another possibility is that an unidentified enzyme binds tunichrome or a thiol as a reducing cofactor to generate V^{III}. Alternatively, an unidentified reductase may facilitate V^{III} formation independently of tunichrome or thiol oxidation. As the bulk of native V^{III} ions in *A. ceratodes* is ligated by water (Carlson, 1975; Tullius et al., 1980; Frank et al., 1995), identification of the native reducing agent presents a formidable challenge. The colorimetric assay for V^{III} utilized here could serve to locate the native reducing agent in fractionated components of blood cells.

ACKNOWLEDGMENT

We are grateful to Ken Kustin for providing a contact to obtain *Ascidia nigra* specimens and for engaging discussions covering broad areas of tunicate inquiry. Tunicates were collected by Dr. Kate Hurlbut.

REFERENCES

Anderson, D. H., & Swinehart, J. H. (1991) *Comp. Biochem. Physiol. 99A*, 585.
Ballhausen, C. J., & Gray, H. B. (1962) *Inorg. Chem. 1*, 111.
Bayer, E., Schiefer, G., Waidelich, D., Scippa, S., & de Vincentiis, M. (1992) *Angew. Chem., Int. Ed. Engl. 31*, 52.
Benfatto, M., Natoli, C. R., Bianconi, A., Garcia, J., Marcelli, A., Fanfoni, M., & Davoli, I. (1986) *Phys. Rev. B. 34*, 33.
Boeri, E., & Ehrenberg, A. (1954) *Arch. Biochem. Biophys. 50*, 404.
Branca, M., Micera, G., Dessì, A., Sanna, D., & Raymond, K. N. (1990) *Inorg. Chem. 29*, 1586.
Brand, S. G., Hawkins, C. J., Marshall, A. T., Nette, G. W., & Parry, D. L. (1989) *Comp. Biochem. Physiol. 93B*, 425.
Bruening, R. C., Oltz, E. M., Furukawa, J., Nakanishi, K., & Kustin, K. (1985) *J. Am. Chem. Soc. 107*, 5298.
Budvari, S. (1989) *The Merck Index*, 3389.
Buglyó, P., Dessì, A., Kiss, T., Micera, G., & Sanna, D. (1993) *J. Chem. Soc., Dalton Trans.*, 2057.
Carlson, R. M. K. (1975) *Proc. Natl. Acad. Sci. U.S.A. 72*, 2217.
Cooper, S. R., Koh, Y. B., & Raymond, K. N. (1982) *J. Am. Chem. Soc. 104*, 5092.
Cramer, S. P., & Hodgson, K. O. (1979) in *Progress in Inorganic Chemistry* (Lippard, S. P., Ed.) Vol. 25, Wiley: New York.
Crouthamel, C. E., Hjelte, B. E., & Johnson, C. E. (1955) *Anal. Chem. 27*, 507.
Degani, H., Gochin, M., Karlish, S. J. D., & Shechter, Y. (1981) *Biochemistry 20*, 5795.
Dingley, A. L., Kustin, K., Macara, I. G., & McLeod, G. C. (1981) *Biochim. Biophys. Acta 649*, 493.
Djuric, S. W. (1984) *J. Org. Chem. 49*, 1311.
Fasman, G. D. (1975) *CRC Handbook of Biochemstry and Molecular Biology I*, CRC Press, Cleveland.
Frank, P., Carlson, R. M. K., & Hodgson, K. O. (1986) *Inorg. Chem. 25*, 470.
Frank, P., Hedman, B., Carlson, R. M. K., Tyson, T. A., Roe, A. L., & Hodgson, K. O. (1987) *Biochemistry 26*, 4975.
Frank, P., Hedman, B., Carlson, R. M. K., & Hodgson, K. O. (1994) *Inorg. Chem. 33*, 3794.
Frank, P., Kustin, K., Robinson, W. E., Linebaugh, L., & Hodgson, K. O. (1995) *Inorg. Chem. 34*, 5942.
George, G. N., Gorbaty, M. L., Keleman, S. R., & Sansone, M. (1991) *Energy Fuels 5*, 93.
Grant, K. B. (1994) Dissertation, Columbia University, New York.
Grant, K. B., Ryan, D. E., Koptyug, I. V., Turro, N. J., & Nakanishi, K. (1996) *J. Inorg. Biochem.* (manuscript in preparation).
Hawkins, C. J., Kott, P., Parry, D. L., & Swinehart, J. H. (1983) *Comp. Biochem. Physiol. 76B*, 555.
Horenstein, B., & Nakanishi, K. (1989) *J. Am. Chem. Soc. 111*, 6242.
Kim, D., Li, Y., Horenstein, B., & Nakanishi, K. (1990) *Tetrahedron Lett. 31*, 7119.
Kim, D., Li, Y., & Nakanishi, K. (1991) *J. Chem. Soc., Chem. Commun.*, 9.
Kosower, E. M. (1976) in *Glutathione: Metabolism and Function* (Arias, I. M., & Jakoby, W. B., Eds.) Raven Press, New York.
Kutzler, F. W., Scott, R. A., Berg. J. M., Hodgson, K. O., Doniach, S., Cramer, S. P., & Chang, C. H. (1981) *J. Am. Chem. Soc. 103*, 6083.
Lee, S., Kustin, K., Robinson, W. E., Frankel, R. B., & Spartalian, K. (1988a) *J. Inorg. Biochem. 33*, 183.
Lee, S., Nakanishi, K., Chiang, M. Y., Frankel, R. B., & Spartalian, K. (1988b) *J. Chem. Soc., Chem. Commun.*, 785.
Lide, D. R. (1993) *CRC Handbook of Chemistry and Physics*, CRC Press, Boca Raton, FL.
Macara, I. G., Kustin, K., & Cantley, L. C. (1980) *Biochim. Biophys. Acta 629*, 95.
Miyanaga, T., Watanabe, I., & Ikeda, S. (1990) *Bull. Chem. Soc. Jpn. 63*, 3282.
Oltz, E. M., Bruening, R. C., Smith, M. J., Kustin, K., & Nakanishi, K. (1988) *J. Am. Chem. Soc. 110*, 6162.
Oltz, E. M., Pollack, S., Delohery, T., Smith, M. J., Ojika, M., Lee, S., Kustin, K., & Nakanishi, K. (1989) *Experientia 45*, 186.
Penner-Hahn, J. E., Benfatto, M., Hedman, B., Takahashi, T., Doniach, S., Groves, J. T., & Hodgson, K. O. (1986) *Inorg. Chem. 25*, 2255.
Pickering, I. J., Brown, G. E., & Tokunaga, T. K. (1995) *Environ. Sci. Tech. 29*, 2456.
Press, W. H., Teukolsky, S. A., Vetterling, W. T., & Flannery, B. P. (1992) in *Numerical Recipes in Fortran*, Cambridge University Press, Cambridge, U.K.
Rezaeva, L. T. (1964) *Zh. Obsch. Biol. 25*, 347 (T836).
Rubinson, K. A. (1981) *Proc. R. Soc. London B 212*, 65.
Ryan, D. E., Ghatlia, N. D., McDermott, A. E., Turro, N. J., Nakanishi, K., & Kustin, K. (1992) *J. Am. Chem. Soc. 114*, 9659.
Ryan, D. E., Grant, K., & Nakanishi, K. (1996) *Biochemistry 35*, 8640−8650.
Shnaiderman, S. Y., Demidovskaya, A. N., & Zaletov, V. G. (1972) *Russ. J. Inorg. Chem. 17*, 348.
Smith, M. J. (1989) *Experientia 45*, 452.
Smith, M. J., Ryan, D. E., Nakanishi, K., Frank, P., & Hodgson, K. O. (1995) in *Metal Ions in Biological Systems 31* (Sigel, H., Ed.) Marcel Dekker, New York.
Taylor, S. W., Molinski, T. F., Rzepecki, L. M., & Waite, J. H. (1991) *J. Nat. Prod. 54*, 918.
Tullius, T. D., Gillum, W. O., Carlson, R. M. K., & Hodgson, K. O. (1980) *J. Am. Chem. Soc. 102*, 5670.
Uyama, T., Moriyama, Y., Futai, M., & Michibata, H. (1994) *J. Exp. Zool. 270*, 148.
Wong, J., Lytle, F. W., Messmer, R. P., & Maylotte, D. H. (1984) *Phys. Rev. B 30*, 5596.
Zolotavin, V. L., Levashova, L. B., & Dolgarev, A. V. (1962) *J. Anal. Chem. USSR 17*, 339.

BI952151Y